Transient analysis of Markov modulated processes with Erlangization, ME-fication and Inverse Laplace transformation*

Miklós Telek
Department of Networked Systems and Services,
Budapest University of Technology and Economics, Hungary
ELKH-BME Information Systems Research Group, Hungary
telek@hit.bme.hu

Abstract

The paper investigates the relation of random clock based and numerical inverse Laplace transformation based transient analysis of Continuous time Markov chains (CTMCs) and Markov fluid models (MFMs) and proves that these methods are identical. This identity leads to new intuitive understanding about the analysis approaches.

Keywords: numerical inverse Laplace transformation, matrix exponential weight function, stochastic model augmented with a random clock.

1 Introduction

For many stochastic models, it is much harder to compute the transient distribution at a given point in time than the stationary distribution. The two main numerical analysis approaches for transient analysis of Markov modulated stochastic models are

- the Laplace transform domain description of the model behaviour and its numerical inverse Laplace transformation (NILT) and

*This work is partially supported by the OTKA K-138208 project and the Artificial Intelligence National Laboratory Programme.

- the introduction of a clock with random delay, whose distribution approximates the time point of interest, and the stationary analysis of the extended stochastic model composed by the original model and the clock.

Both of these approaches are based on *weight functions*, which characterize the numerical properties of the methods. In case of the random clock based methods, the weight functions are the density functions of the clock distributions.

These two analysis methods are considered to be essentially different by the majority of the stochastic modelling community. For example, exact Laplace domain description based NILT is typically considered to be "exact", while the random clock based methods are commonly assumed to be "approximate". The different perceptions of these methods are also related with the typical weight functions applied by the two approaches. In clock augmented stochastic models, the weight function of the clock is non-negative. Random clock methods with a potentially negative weight function is perceived to be "dirty hack", while NILT is considered to be "valid" in spite of the fact that the weight functions of the most common NILT methods (e.g., Euler method [2], Gaver method [16]) have alternating signs.

Furthermore, the weight functions of many NILT methods exhibit amplified waving behaviour with increasing order (most dominantly the Euler method), while the typical weight functions of the clock augmented models (e.g. Erlang density function) nicely converge to the unit impulse. This way, the random clock based approach is considered to be "asymptotically correct", while the NILT based analysis is considered to be "numerically unstable" with increasing order.

Considering Continuous time Markov chains (CTMCs) and Markov fluid models (MFMs), the paper proves the identity of these two approaches for the most common case, when the weight functions of the NILT method and the random clock method are matrix exponential functions. We conjecture that the identity of these analysis approaches extends to more stochastic processes, but the focus of the present paper is restricted to CTMCs and MFMs.

The class of NILT methods with matrix exponential weight functions (MEWFs) is not exhaustive but it contains the most efficient methods, e.g. the methods of the Abate-Whitt framework [2] (e.g., Euler method [1], Gaver method [16], Talbot method [17], CME method [12]) as well as NILT methods based on the derivatives of the Laplace transform function.

The random clock based analysis approach has been introduced in [18], and has been efficiently used for the transient analysis of quasi birth death

processes [19] and MFMs [5]. The weight functions of the random clock based analysis literature are exclusively matrix exponential functions. The case when the clock is Erlang distributed is commonly referred to as Erlangization [15], and when the clock is concentrated matrix exponential distributed is referred to as ME-fication [5].

The rest of the paper is organized as follows. Section 2 introduces a general framework using MEWFs, and it explains the role of the weight function in the NILT and in the random clock based analysis method. As a simple application of the introduced framework, Section 3 proves the identity of the two analysis approaches for CTMCs. The same identity of the two approaches is proved for a more complex Markov modulated stochastic process, the MFM, in Section 4. Section 5 concludes the paper.

2 The general framework

This section introduces a MEWF based approximate analysis of a function at (time) t. It discusses the two main cases, when the matrix of the MEWF is diagonalizable and non-diagonalizable. The last two subsections explain the relation of the NILT and the random clock based approach with the approximate analysis using MEWFs.

2.1 Weight function based approximate analysis of $\mathbf{h}(t)$

Let $\mathbf{h}(t)$ be a matrix valued function ($\mathbf{h} : \mathcal{R}^1 \to \mathcal{R}^{n_1 \times n_2}$). There are many practically interesting cases when $\mathbf{h}(T)$ is hard/not possible to compute, but

$$\mathbf{h}_N(T) = \int_{t=0}^{\infty} \mathbf{h}(Tt) f_N(t) dt = \int_{t=0}^{\infty} \mathbf{h}(t) f_N(t/T)/T dt \tag{1}$$

can be computed, where

$$f_N(t) = \boldsymbol{\alpha} e^{\mathbf{A}t} \boldsymbol{a} \tag{2}$$

is a real MEWF with $\boldsymbol{a} = -\mathbf{A}\mathbb{1}$ and $\mathbb{1}$ is the column vector of ones. The size of row vector $\boldsymbol{\alpha}$ and column vector $\mathbb{1}$ is N and the size of matrix $\mathbf{A}$ is $N \times N$. $f_N(t)$ is *Markovian* when $\boldsymbol{\alpha} \geq 0$, $\boldsymbol{a} \geq 0$ and the off-diagonal elements of $\mathbf{A}$ are non-negative. We assume that the eigenvalues of $\mathbf{A}$ have negative real parts, the $f_N(t)$ weight function is *normalized* (i.e., $\int_0^\infty f_N(t)dt = 1$) and is *centered* at one (i.e., $\int_0^\infty t f_N(t)dt = 1$). $\boldsymbol{\alpha}\mathbb{1} = 1$ ensures that $f_N(t)$ is normalized. Intuitively, when $f_N(t)$ is a close approximate (in some sense) of the Dirac impulse function at one then $\mathbf{h}_N(T)$ is a close approximate of $\mathbf{h}(T)$.

If $f_N(t)$ is normalized and is centered at one, then $f_N(t/T)/T = \boldsymbol{\alpha} e^{\mathbf{A}t/T}\boldsymbol{a}/T$ is a normalized MEWF ($\int_0^\infty f_N(t/T)/T dt = 1$), which is centered at T ($\int_0^\infty t f_N(t/T)/T dt = T$). We interchangeably use the two integrals of (1) in the sequel.

Based on the spectral decomposition of $\mathbf{A}$, with eigenvalues $-\beta_i$, we have the following two cases.

- If $\mathbf{A}$ is not diagonalizable, then $f_N(t)$ can be written as

$$f_N(t) = \boldsymbol{\alpha} e^{\mathbf{A}t}\boldsymbol{a} = \sum_{i=1}^{\#\beta}\sum_{j=1}^{\#\beta_i} \eta_{ij} t^{j-1} e^{-\beta_i t}, \tag{3}$$

  where $\#\beta$ is the number of different eigenvalues of $\mathbf{A}$, and $\#\beta_i$ is the multiplicity of eigenvalue β_i. That is $\sum_{i=1}^{\#\beta} \#\beta_i = N$.

- If $\mathbf{A}$ is diagonalizable, then

$$f_N(t) = \boldsymbol{\alpha} e^{\mathbf{A}t}\boldsymbol{a} = \sum_{n=1}^{N} \eta_n e^{-\beta_n t}. \tag{4}$$

Since $\boldsymbol{\alpha} e^{\mathbf{A}t}\boldsymbol{a}$ is real, the β_n eigenvalues and the associated coefficients are real or complex conjugate pairs.

2.2 Special weight functions

MEWF	ref.	eigenvalue	sign	diagonalizable	Markovian
Euler	[2]	complex	alternating	yes	no
CME	[11]	complex	non-negative	yes	no
Gaver	[16]	real	alternating	yes	no
CMER	[13]	real	non-negative	no	no
Erlang	[6]	real	positive	no	yes

Table 1: Classification of the most efficient MEWFs

Table 1 presents a classification of the most efficient MEWFs applied in NILT and random clock methods. We refer to [11] and [13] for more detailed comparisons of these MEWFs. The following subsections provide further details on the Erlang and the CME MEWFs, as representatives of MEWFs with non-diagonalizable and diagonalizable matrices, respectively.

2.2.1 Erlangization

The transient analysis method with Erlang distributed weight function is commonly referred to as Erlangization [15]. The order N Erlang distributed weight function has the form

$$f_N^{Erl}(t) = \frac{N^N t^{N-1} e^{-Nt}}{(N-1)!}, \tag{5}$$

which is normalized and centralized at one. This $f_N(t)$ function has the following two representations.

According to (2), $f_N^{Erl}(t) = \boldsymbol{\alpha} e^{\mathbf{A}t} \boldsymbol{a}$ with

$$\boldsymbol{\alpha} = \boldsymbol{e_1} \text{ and } \mathbf{A} = \begin{bmatrix} -N & N & & \\ & -N & N & \\ & & \ddots & \ddots \\ & & & -N \end{bmatrix}, \tag{6}$$

where $\boldsymbol{e_k}$ denotes the kth unit vector, and according to (3), $f_N^{Erl}(t) = \sum_{i=1}^{\#\beta} \sum_{j=1}^{\#\beta_i} \eta_{ij} t^{j-1} e^{-\beta_i t}$ with

$$\#\beta = 1, \quad \#\beta_1 = N, \quad \beta_1 = N, \quad \eta_{1j} = \begin{cases} 0 & \text{if } j < N, \\ \frac{N^N}{(N-1)!} & \text{if } j = N. \end{cases} \tag{7}$$

That is, the Erlang distributed weight function is an example of the case when $\mathbf{A}$ is not diagonalizable.

2.2.2 ME-fication

The transient analysis method with concentrated non-negative MEWF is referred to as ME-fication in [5]. For odd N, such MEWF has the form

$$f_N(t) = c\, e^{-\lambda t} \prod_{j=1}^{(N-1)/2} \cos^2\left(\frac{\omega\lambda t - \phi_j}{2}\right), \tag{8}$$

which is non-negative by construction. For a given setting of the $\omega, \phi_1, \ldots, \phi_{(N-1)/2}$ parameters, c and λ are set to make $f_N(t)$ normalized and centered at one. Based on a trigonometric-exponential transformation [11], $f_N(t)$ can also be written in the following two forms

$$f_N(t) = c\, e^{-\lambda t} \prod_{j=1}^{(N-1)/2} \cos^2\left(\frac{\omega\lambda t - \phi_j}{2}\right) = \sum_{n=1}^{N} \eta_n e^{-\beta_n t} = \boldsymbol{\alpha} e^{\mathbf{A}t} \boldsymbol{a}, \tag{9}$$

with $\boldsymbol{\alpha} = \left[\frac{\eta_1}{\beta_1}, \frac{\eta_2}{\beta_2}, \ldots, \frac{\eta_N}{\beta_N}\right]$ and $\mathbf{A} = \text{Diag}\langle -\beta_n \rangle$. That is, in this case, $f_N(t)$ is also a matrix exponential function, but matrix $\mathbf{A}$ is diagonalizable.

2.3 Inverse Laplace transformation

One of the most generic cases when $\mathbf{h}(T)$ is not possible to compute but (1) can be computed, is the case when only the Laplace transform (LT) of $\mathbf{h}(t)$,

$$\mathbf{h}^*(s) = \int_{t=0}^{\infty} e^{-st}\mathbf{h}(t)\mathrm{d}t, \tag{10}$$

is known and we are interested in $\mathbf{h}(T)$. Assuming that the symbolic inverse LT of $\mathbf{h}^*(s)$ is not available, NILT needs to be applied to approximate $\mathbf{h}(T)$.

For later use, we also define the matrix generalization of the Laplace transform as

$$\mathbf{H}^*(\mathbf{M}) = \int_{t=0}^{\infty} \mathbf{h}(t) \otimes e^{-\mathbf{M}t}\mathrm{d}t = \int_{t=0}^{\infty} \mathbf{h}(t) \otimes \sum_{k=0}^{\infty} \frac{(-t)^k}{k!}\mathbf{M}^k\mathrm{d}t, \tag{11}$$

where $\mathbf{M}$ is a square matrix of size N and $\otimes$ denotes the Kronecker product. That is, $\mathbf{H}^* : \mathcal{R}^{N\times N} \to \mathcal{R}^{n_1 N\times n_2 N}$.

2.3.1 NILT using Abate-Whitt framework methods

The most commonly applied NILT methods belong to the, so called, Abate-Whitt framework [2]. According to this framework, the order N approximate of $\mathbf{h}(t)$ at point T is obtained based on $\mathbf{h}^*(s)$ as

$$\mathbf{h}(T) \approx \mathbf{h}_N(T) := \sum_{n=1}^{N} \frac{\eta_n}{T}\mathbf{h}^*\left(\frac{\beta_n}{T}\right), \tag{12}$$

where the coefficients η_n and β_n are determined by the order (N) and the NILT method (e.g., Euler [1], Gaver [16], Talbot [17], CME [12]) and they are independent of the function $\mathbf{h}^*(s)$. Substituting (10) into (12) gives

$$\mathbf{h}_N(T) = \int_0^{\infty} \mathbf{h}(tT) \cdot f_N(t)\mathrm{d}t, \tag{13}$$

where

$$f_N(t) = \sum_{n=1}^{N} \eta_n e^{-\beta_n t} = \boldsymbol{\alpha} e^{\mathbf{A}t}\boldsymbol{a}, \tag{14}$$

with $\boldsymbol{\alpha} = \left[\frac{\eta_1}{\beta_1}, \frac{\eta_2}{\beta_2}, \ldots, \frac{\eta_N}{\beta_N}\right]$ and $\mathbf{A} = \mathrm{Diag}\langle -\beta_n\rangle$.

That is, the Abate-Whitt framework methods are associated with MEWFs whose matrix $\mathbf{A}$ is diagonalizable.

2.3.2 NILT using the derivatives of the Laplace transform

Some NILT methods, which are not part of the Abate-Whitt framework, evaluate also the derivatives of the Laplace transform function for NILT [9, 1] (see [12, Sec. 4.2] for a recent summary) as follows

$$\mathbf{h}(T) \approx \mathbf{h}_N(T) := \sum_{i=1}^{\#\beta} \sum_{j=1}^{\#\beta_i} \frac{1}{(-T)^{j-1}} \frac{\eta_{ij}}{T} \frac{d^{j-1}}{ds^{j-1}} \mathbf{h}^*(s) \Big|_{s=\frac{\beta_i}{T}}, \tag{15}$$

where $\#\beta$ is the number of different values at which the LT function and its derivatives are evaluated and $\#\beta_i - 1$ is the highest derivative of the LT function which is evaluated at point β_i. The overall number of evaluations of the LT function and its derivatives is $\sum_{i=1}^{\#\beta} \#\beta_i = N$.

Based on the definition of the Laplace transform in (10), we have

$$\frac{d^n}{ds^n}\mathbf{h}^*(s) = \int_{t=0}^{\infty} \frac{d^n}{ds^n} e^{-st}\mathbf{h}(t)\mathrm{d}t = \int_{t=0}^{\infty} (-t)^n e^{-st}\mathbf{h}(t)\mathrm{d}t. \tag{16}$$

From which, (15) takes the form

$$\begin{aligned} \mathbf{h}_N(T) &= \sum_{i=1}^{\#\beta} \sum_{j=1}^{\#\beta_i} \frac{1}{(-T)^{j-1}} \frac{\eta_{ij}}{T} \int_{t=0}^{\infty} (-t)^{j-1} e^{-t\beta_i/T}\mathbf{h}(t)\mathrm{d}t \\ &= \int_0^{\infty} \mathbf{h}(t) \cdot \frac{1}{T} f_N(t/T)\mathrm{d}t = \int_0^{\infty} \mathbf{h}(tT) \cdot f_N(t)\mathrm{d}t, \end{aligned} \tag{17}$$

where

$$f_N(t) = \sum_{i=1}^{\#\beta} \sum_{j=1}^{\#\beta_i} \eta_{ij} t^{j-1} e^{-\beta_i t}.$$

Consequently, NILT methods using the derivatives of the Laplace transform are associated with MEWFs whose matrix $\mathbf{A}$ is non-diagonalizable.

The most common application of NILT using the derivatives of the Laplace transform is the case of Erlang weight function, when the parameters of (15) are set according to (7). In this case,

$$\mathbf{h}(T) \approx \mathbf{h}_N^{Erl}(T) := \frac{1}{(-T)^{N-1}} \frac{\frac{N^N}{(N-1)!}}{T} \frac{d^{N-1}}{ds^{N-1}} \mathbf{h}^*(s) \Big|_{s=\frac{N}{T}}. \tag{18}$$

Utilizing (16) again, it can be re-written as

$$\begin{aligned} \mathbf{h}_N^{Erl}(T) &= \frac{1}{(-T)^{N-1}} \frac{N^N}{(N-1)!T} \int_{t=0}^{\infty} (-t)^{N-1} e^{-tN/T}\mathbf{h}(t)\mathrm{d}t \\ &= \int_{t=0}^{\infty} \frac{1}{T} \frac{N^N (t/T)^{N-1}}{(N-1)!} e^{-tN/T}\mathbf{h}(t)\mathrm{d}t = \int_0^{\infty} \frac{1}{T} f_N^{Erl}(t/T)\mathbf{h}(t)\mathrm{d}t, \end{aligned} \tag{19}$$

where $f_N^{Erl}(t)$ is the order N Erlang density function concentrated at one, which be represented according to (5) and (6).

2.3.3 NILT with matrix exponential weight functions

The two special cases presented in the previous subsections can be summarized in the following general theorem.

Theorem 1. *Let $f_N(t) = \boldsymbol{\alpha} e^{\mathbf{A}t} \boldsymbol{a}$ be a normalized MEWF which is centered at one. The NILT approximation of matrix $\mathbf{h}(T)$ of size $n_1 \times n_2$ using the MEWF $f_N(t)$ is*

$$\mathbf{h}(T) \approx \mathbf{h}_N(T) = \int_{t=0}^{\infty} \mathbf{h}(Tt) f_N(t) dt = (\mathbf{I}_{n_1} \otimes \boldsymbol{\alpha})\ \mathbf{H}^*(-\mathbf{A}/T)\ (\mathbf{I}_{n_2} \otimes \boldsymbol{a}/T), \tag{20}$$

where $\mathbf{I}_n$ denotes the unity matrix of size n.

Proof. Using (11), we have

$$(\mathbf{I}_{n_1} \otimes \boldsymbol{\alpha})\ \mathbf{H}^*(-\mathbf{A}/T)\ (\mathbf{I}_{n_2} \otimes \boldsymbol{a}/T) = (\mathbf{I}_{n_1} \otimes \boldsymbol{\alpha}) \int_{t=0}^{\infty} \mathbf{h}(t) \otimes e^{t\mathbf{A}/T} \mathrm{d}t\ (\mathbf{I}_{n_2} \otimes \boldsymbol{a}/T)$$
$$= \int_{t=0}^{\infty} \mathbf{h}(t) \cdot \boldsymbol{\alpha} e^{t\mathbf{A}/T} \boldsymbol{a}/T \mathrm{d}t = \int_{t=0}^{\infty} \mathbf{h}(t)\ f_N(t/T)/T \mathrm{d}t = \int_{t=0}^{\infty} \mathbf{h}(tT)\ f_N(t) \mathrm{d}t.$$

□

The above discussed two special cases, the case when $\mathbf{A}$ is diagonalizable and the case when $f_N(t) = f_N^{Erl}(t)$ can be obtained as follow.

A is diagonalizable

When $\boldsymbol{\alpha} = \left[\frac{\eta_1}{\beta_1}, \frac{\eta_2}{\beta_2}, \ldots, \frac{\eta_N}{\beta_N}\right]$ and $\mathbf{A} = \mathrm{Diag}\langle -\beta_n \rangle$, then $f_N(t) = \sum_{n=1}^{N} \eta_n e^{-\beta_n t}$ and from Theorem 1 we have

$$(\mathbf{I}_{n_1} \otimes \boldsymbol{\alpha})\ \mathbf{H}^*(-\mathbf{A}/T)\ (\mathbf{I}_{n_2} \otimes \boldsymbol{a}/T) = \int_{t=0}^{\infty} \mathbf{h}(t)\ f_N(t/T)/T \mathrm{d}t$$
$$= \int_{t=0}^{\infty} \mathbf{h}(t)\ \sum_{n=1}^{N} \frac{\eta_n}{T} e^{-\beta_n t/T} \mathrm{d}t = \sum_{n=1}^{N} \frac{\eta_n}{T}\ \mathbf{h}^*\left(\frac{\beta_n}{T}\right).$$

A is composed of a single Jordan block

When $\boldsymbol{\alpha}$ and $\mathbf{A}$ are defined according to (6), then $\boldsymbol{a} = -\mathbf{A}\mathbb{1} = [0,\ldots,0,N]^T = N\boldsymbol{e_N}^T$ and the Jordan decomposition of $-\mathbf{A}/T$ has the form

$$\underbrace{\begin{bmatrix}(-T/N)^0 & & & \\ & (-T/N)^1 & & \\ & & \ddots & \\ & & & (-T/N)^{N-1}\end{bmatrix}}_{\mathbf{S}^{-1}} \cdot \underbrace{\begin{bmatrix}N/T & 1 & & \\ & N/T & 1 & \\ & & \ddots & \ddots \\ & & & N/T\end{bmatrix}}_{\mathbf{J}_N(N/T)} \cdot \underbrace{\begin{bmatrix}(-N/T)^0 & & & \\ & (-N/T)^1 & & \\ & & \ddots & \\ & & & (-N/T)^{N-1}\end{bmatrix}}_{\mathbf{S}}, \quad (21)$$

where $\mathbf{J}_n(\lambda)$ denotes the size n Jordan block of eigenvalue λ. Based on this decomposition of $-\mathbf{A}/T$, we write

$$\begin{aligned}
&(\mathbf{I}_{n_1} \otimes \boldsymbol{\alpha})\ \mathbf{H}^*(-\mathbf{A}/T)\ (\mathbf{I}_{n_2} \otimes \boldsymbol{a}/T) = \int_{t=0}^{\infty} \mathbf{h}(t) \cdot \boldsymbol{\alpha} e^{t\mathbf{A}/T} \boldsymbol{a}/T \mathrm{d}t \\
&= \int_{t=0}^{\infty} \mathbf{h}(t) \cdot N/T \boldsymbol{e_1} \mathbf{S}^{-1} e^{-t\mathbf{J}_N(N/T)} \mathbf{S} \boldsymbol{e_N}^T \mathrm{d}t \\
&= \int_{t=0}^{\infty} \mathbf{h}(t) \cdot N/T(-N/T)^{N-1} \boldsymbol{e_1} e^{-t\mathbf{J}_N(N/T)} \boldsymbol{e_N}^T \mathrm{d}t \\
&= N/T(-N/T)^{N-1} (\mathbf{I}_{n_1} \otimes \boldsymbol{e_1})\ \mathbf{h}^*(\mathbf{J}_N(N/T))\ (\mathbf{I}_{n_2} \otimes \boldsymbol{e_N}^T) \\
&= (-1)^{N-1} \frac{N^N}{T^N} \frac{1}{(N-1)!} \frac{d^{N-1}}{ds^{N-1}} \mathbf{h}^*(s)\big|_{s=N/T}, \qquad (22)
\end{aligned}$$

where we used $\mathbf{H}^*(-\mathbf{A}/T) = \mathbf{H}^*(\mathbf{S}^{-1}\mathbf{J}\mathbf{S}) = (\mathbf{I}_{n_1} \otimes \mathbf{S}^{-1})\mathbf{H}^*(\mathbf{J})(\mathbf{I}_{n_2} \otimes \mathbf{S})$ in the second step and

$$\mathbf{H}^*(\mathbf{J}_N(\lambda)) = \begin{bmatrix}\mathbf{h}^*(\lambda) & \mathbf{h}^{*\prime}(\lambda)/1! & \mathbf{h}^{*\prime\prime}(\lambda)/2! & \cdots & \mathbf{h}^{*(N-1)}(\lambda)/(N\text{–}1)! \\ & \mathbf{h}^*(\lambda) & \mathbf{h}^{*\prime}(\lambda)/1! & \ddots & \vdots \\ & & \ddots & \ddots & \vdots \\ & & & \mathbf{h}^*(\lambda) & \mathbf{h}^{*\prime}(\lambda)/1! \\ & & & & \mathbf{h}^*(\lambda)\end{bmatrix},$$

from [10], in the last step. The expression obtained in (22) is identical with (18).

In summary, when $\mathbf{A}$ is diagonalizable it is enough to compute $\mathbf{h}^*(s)$ with scalar parameters (which are the eigenvalues of $\mathbf{A}$), while in general, we need to compute $\mathbf{H}^*(-\mathbf{A}/T)$ with matrix parameter if $\mathbf{A}$ is not diagonalizable. We distinguish these two cases also in the sequel.

2.4 Stochastic models augmented with a random clock

The random clock based analysis approach is introduced in [18]. Its main steps are as follows:

- augment the stochastic model with a random clock, whose density function approximates the unit impulse at the time instant of interest,
- start the stochastic model and the clock,
- when the clock expires reset both the clock and the stochastic model to its initial state, and continue these cycles forever,
- evaluate the stationary distribution of this cyclic model,
- based on the stationary distribution of the cyclic model compute the distribution of the stochastic model at the embedded clock instances.

The application details of this analysis approach are provided in the following sections for different stochastic processes.

3 Transient analysis of CTMC

The transient analysis of CTMCs is rather well established. In spite of that, in this section we consider the NILT and random clock based analysis approaches of CTMCs and prove the following theorem.

Theorem 2. *Consider the transient distribution of the CTMC with initial probability vector $\boldsymbol{\pi}$ and generator $\mathbf{Q}$ at time T. The numerical computations of this transient distribution with the random clock method and with NILT are identical when the same MEWF, $f_N(t) = \boldsymbol{\alpha} e^{\mathbf{A}t}\boldsymbol{a}$, is used.*

Proof. In the following subsections, we show that the random clock based analysis approach results in (30), while the NILT based analysis results in (39), which are identical. □

3.1 Background

For a CTMC, $X(t) \in \mathcal{S}$, with $S = |\mathcal{S}|$ states ($S < \infty$), generator $\mathbf{Q}$ and initial probability vector $\boldsymbol{\pi}$, the evolution of the transient probability vector, $\boldsymbol{p}(t)$, whose jth element is $p_j(t) = \Pr(X(t) = j)$, is governed by the ordinary differential equation

$$\frac{d}{dt}\boldsymbol{p}(t) = \boldsymbol{p}(t)\mathbf{Q}, \quad \text{with initial value } \boldsymbol{p}(0) = \boldsymbol{\pi}. \tag{23}$$

The solution of (23) is

$$\boldsymbol{p}(t) = \boldsymbol{\pi} e^{\mathbf{Q}t} = \boldsymbol{\pi} \sum_{k=0}^{\infty} \frac{t^k}{k!} \mathbf{Q}^k. \tag{24}$$

The most common way to compute $\boldsymbol{p}(T)$ is via (24), but in this paper we focus on the NILT and the random clock based methods.

3.1.1 Laplace transform domain description

The LT of $\boldsymbol{p}(T)$ is

$$\boldsymbol{p}^*(s) = \int_0^{\infty} e^{-st} \boldsymbol{p}(t) dt = \boldsymbol{\pi}(s\mathbf{I} - \mathbf{Q})^{-1}. \tag{25}$$

3.1.2 Stationary distribution

When $\mathbf{Q}$ is the generator of an irreducible CTMC, then $\mathbf{Q}\mathbb{1} = \mathbf{0}$, that is, zero is an eigenvalue of $\mathbf{Q}$, and the other $S-1$ eigenvalues of $\mathbf{Q}$ have negative real parts. In this case, $\boldsymbol{p}(t)$ converges to the stationary distribution of the CTMC, $\boldsymbol{p} = \lim_{t\to\infty} \boldsymbol{p}(t)$, which is a proper probability distribution ($\boldsymbol{p}$ is non-negative and $\boldsymbol{p}\mathbb{1} = 1$). The stationary distribution, $\boldsymbol{p}$, can be obtained as the solution of the linear system $\boldsymbol{p}\mathbf{Q} = \mathbf{0},\ \boldsymbol{p}\mathbb{1} = 1$.

3.1.3 Transient CTMC

When $\mathbf{Q}$ is a transient generator of a CTMC, then all eigenvalues of $\mathbf{Q}$ have negative real parts and $\boldsymbol{p}(t)$ converges to $\lim_{t\to\infty} \boldsymbol{p}(t) = \mathbf{0}$.

For the treatment of the transient case, we define $\tilde{\boldsymbol{p}}(t) = \int_{\tau=0}^{t} \boldsymbol{p}(\tau)\mathrm{d}\tau$. Integrating (23) from 0 to t, we obtain that $\tilde{\boldsymbol{p}}(t)$ satisfies

$$\frac{d}{dt}\tilde{\boldsymbol{p}}(t) = \boldsymbol{\pi} + \tilde{\boldsymbol{p}}(t)\mathbf{Q}, \quad \text{with initial value } \tilde{\boldsymbol{p}}(0) = \mathbf{0}. \tag{26}$$

In this case, $\tilde{\boldsymbol{p}}(t)$ converges to $\tilde{\boldsymbol{p}}(\infty) = \lim_{t\to\infty} \tilde{\boldsymbol{p}}(t) = \int_{\tau=0}^{\infty} \boldsymbol{p}(\tau)\mathrm{d}\tau$, which is the solution of $\mathbf{0} = \boldsymbol{\pi} + \tilde{\boldsymbol{p}}(\infty)\mathbf{Q}$ (obtained from (26) at the $t \to \infty$ limit). That is

$$\tilde{\boldsymbol{p}}(\infty) = \boldsymbol{\pi}(-\mathbf{Q})^{-1}, \tag{27}$$

where $\mathbf{Q}$ is non-singular, since its eigenvalues have negative real parts.

3.2 CTMC augmented with a random clock

In this subsection, we approximate $\boldsymbol{p}(T)$ with the random clock approach and denote the result with $\boldsymbol{p}^{(N)}(T)$. To compute $\boldsymbol{p}^{(N)}(T)$, we extend the CTMC with a random clock whose weight function is $f_N(t/T)/T = \boldsymbol{\alpha} e^{\mathbf{A}t/T}\boldsymbol{a}/T$, where $f_N(t/T)/T$ is normalized and centralized at T. Extending the CTMC with the random clock, results in an extended CTMC process, $\hat{X}(t)$, with generator

$$\hat{\mathbf{Q}} = \begin{array}{|c|c|} \hline \mathbf{Q} \oplus \mathbf{A}/T & \mathbb{1} \otimes \boldsymbol{a}/T \\ \hline \boldsymbol{\pi} \otimes \boldsymbol{\alpha} & -1 \\ \hline \end{array}.$$

If $\boldsymbol{\alpha}$, $\boldsymbol{a}$ and the non-diagonal elements of $\mathbf{A}$ are non-negative, then the extended process is a CTMC as well, but we do not assume this property in the current paper.

The $\hat{\mathbf{Q}}$ generator describes the process evolution on a state space of size $SN + 1$. The first SN states describe the parallel evolution of the original CTMC and the clock, and the last state is used to reset the CTMC into its initial distribution and to reset the clock. The time to reset the model is exponentially distributed with parameter one. Since the performance measure of interest of the random clock method is the behaviour of the process at embedded clock points, the particular choice of the reset time parameter does not play any role. The stationary vector of this extended model, $\hat{\boldsymbol{p}} = [\bar{\boldsymbol{p}}, p^{\triangle}]$ (where vector $\bar{\boldsymbol{p}}$ is of size SN and $p^{\triangle}$ is a scalar), is the solution of the linear system

$$\hat{\boldsymbol{p}}\hat{\mathbf{Q}} = \mathbf{0}, \quad \hat{\boldsymbol{p}}\mathbb{1} = 1.$$

According to the block structure of $\hat{\mathbf{Q}}$, $\bar{\boldsymbol{p}}$ satisfies

$$\bar{\boldsymbol{p}}(\mathbf{Q} \oplus \mathbf{A}/T) + p^{\triangle}(\boldsymbol{\pi} \otimes \boldsymbol{\alpha}) = \mathbf{0}, \tag{28}$$

from which

$$\bar{\boldsymbol{p}} = -p^{\triangle}(\boldsymbol{\pi} \otimes \boldsymbol{\alpha})(\mathbf{Q} \oplus \mathbf{A}/T)^{-1}. \tag{29}$$

We note that $\mathbf{Q} \oplus \mathbf{A}$ is a transient generator, since the eigenvalues of $\mathbf{Q}$ have non-positive real parts and the eigenvalues of $\mathbf{A}$ have negative real parts, consequently, all eigenvalues of $\mathbf{Q} \oplus \mathbf{A}$ have negative real parts.

Theorem 3. *The stationary embedded distribution of the original CTMC at a clock event is*

$$\boldsymbol{p}^{(N)} = -(\boldsymbol{\pi} \otimes \boldsymbol{\alpha})(\mathbf{Q} \oplus \mathbf{A}/T)^{-1}(\mathbf{I} \otimes \boldsymbol{a}/T). \tag{30}$$

Proof. The distribution of the original CTMC at a clock event can be computed as

$$\begin{aligned} p_i^{(N)} &= \lim_{t\to\infty}\lim_{\delta\to 0}\frac{\Pr(\hat{X}(t)=\{i,\cdot\} \text{ and the clock expires in } (t,t+\delta)\ )}{\Pr(\text{the clock expires in } (t,t+\delta))} \\ &= \lim_{t\to\infty}\lim_{\delta\to 0}\frac{\sum_{n=1}^{N}\Pr(\hat{X}(t)=\{i,n\})(a_n\delta/T+\sigma(\delta))}{\sum_{k=1}^{S}\sum_{n=1}^{N}\Pr(\hat{X}(t)=\{k,n\})(a_n\delta/T+\sigma(\delta))} \\ &= \lim_{t\to\infty}\frac{\sum_{n=1}^{N}\Pr(\hat{X}(t)=\{i,n\})a_n/T}{\sum_{k=1}^{S}\sum_{n=1}^{N}\Pr(\hat{X}(t)=\{k,n\})a_n/T} = \frac{\sum_{n=1}^{N}\bar{p}_{i,n}a_n/T}{\sum_{k=1}^{S}\sum_{n=1}^{N}\bar{p}_{k,n}a_n/T}, \end{aligned}$$

where $\sigma(\cdot)$ is an error term such that $\lim_{\delta\to 0}\sigma(\delta)/\delta = 0$, and a_n denotes the n^{th} entry of vector $\boldsymbol{a}$. The vector composed of these elements, $\boldsymbol{p}^{(N)} = \{p_i^{(N)}\}$, can be written as

$$\boldsymbol{p}^{(N)} = \frac{\bar{\boldsymbol{p}}(\mathbf{I}\otimes\boldsymbol{a}/T)}{\bar{\boldsymbol{p}}(\mathbb{1}\otimes\boldsymbol{a}/T)} = \frac{-(\boldsymbol{\pi}\otimes\boldsymbol{\alpha})(\mathbf{Q}\oplus\mathbf{A}/T)^{-1}(\mathbf{I}\otimes\boldsymbol{a}/T)}{-(\boldsymbol{\pi}\otimes\boldsymbol{\alpha})(\mathbf{Q}\oplus\mathbf{A}/T)^{-1}(\mathbb{1}\otimes\boldsymbol{a}/T)}, \tag{31}$$

where we substituted (29) in the second step. To simplify the denominator, we write

$$\begin{aligned} (\mathbf{Q}\oplus\mathbf{A}/T)(\mathbb{1}\otimes\mathbb{1}) &= (\mathbf{Q}\otimes\mathbf{I})(\mathbb{1}\otimes\mathbb{1}) + (\mathbf{I}\otimes\mathbf{A}/T)(\mathbb{1}\otimes\mathbb{1}) &(32)\\ &= \mathbf{0}\otimes\mathbb{1} - \mathbb{1}\otimes\boldsymbol{a}/T = -\mathbb{1}\otimes\boldsymbol{a}/T, &(33)\end{aligned}$$

from which $-(\mathbf{Q}\oplus\mathbf{A}/T)^{-1}(\mathbb{1}\otimes\boldsymbol{a}/T) = (\mathbb{1}\otimes\mathbb{1})$. Using this, the denominator of (31) becomes $(\boldsymbol{\pi}\otimes\boldsymbol{\alpha})(\mathbb{1}\otimes\mathbb{1}) = 1$, which results in the statement of the theorem. □

3.3 Transient analysis with NILT

In this subsection, we approximate $\boldsymbol{p}(T)$ with NILT and denote the results with $\boldsymbol{p}_N(T)$.

3.3.1 NILT when A is diagonalizable

When $\mathbf{A}$ is diagonalizable, the Abate-Whitt framework method with coefficients η_n and β_n approximates the transient probability vector of the CTMC at time T, based on its LT, $\boldsymbol{p}^*(s)$, as follows

$$\boldsymbol{p}(T) \approx \boldsymbol{p}_N(T) = \sum_{n=1}^{N}\frac{\eta_n}{T}\boldsymbol{p}^*\left(\frac{\beta_n}{T}\right) = \sum_{n=1}^{N}\frac{\eta_n}{T}\boldsymbol{\pi}\left(\frac{\beta_n}{T}\mathbf{I}-\mathbf{Q}\right)^{-1}. \tag{34}$$

3.3.2 NILT when A is not diagonalizable

When $\mathbf{A}$ is not diagonalizable, Theorem 1 can be used to approximate $\boldsymbol{p}(T)$, which requires the computation of $\mathbf{P}^*(-\mathbf{A}/T) = \int_0^\infty \boldsymbol{p}(t) \otimes e^{\mathbf{A}t/T} dt$. In the special case of CTMCs, direct methods can compute $\mathbf{P}^*(-\mathbf{A}/T)$ based on (24), but to introduce an analysis approach which is applicable for more complex Markov modulated models, we utilize only (23).

Theorem 4. *When $\boldsymbol{p}(t)$ satisfies (23) then*

$$\mathbf{P}^*(-\mathbf{A}/T) = -(\boldsymbol{\pi} \otimes \mathbf{I}_N)(\mathbf{Q} \oplus \mathbf{A}/T)^{-1}. \tag{35}$$

Proof. Let $\mathbf{v}(t) = \mathbf{p}(t) \otimes \mathbf{u}(t)$, where $\mathbf{u}(t)$ of size $N \times N$ satisfies the ODE

$$\frac{d}{dt}\mathbf{u}(t) = \mathbf{u}(t)\ \mathbf{A}/T, \text{ with initial value } \mathbf{u}(0) = \mathbf{I}_N. \tag{36}$$

On the one hand, $\mathbf{u}(t) = e^{t\mathbf{A}/T}$ from the solution of (36). On the other hand, $\mathbf{v}(t)$ satisfies

$$\frac{d}{dt}\mathbf{v}(t) = \mathbf{v}(t)(\mathbf{Q} \oplus \mathbf{A}/T), \text{with initial value } \mathbf{v}(0) = \boldsymbol{\pi} \otimes \mathbf{I}_N, \tag{37}$$

according to (23) and (36). Similar to (26), $\tilde{\boldsymbol{v}}(t) = \int_{\tau=0}^{t} \boldsymbol{v}(\tau)\mathrm{d}\tau$ satisfies

$$\frac{d}{dt}\tilde{\mathbf{v}}(t) = \mathbf{v}(0) + \tilde{\mathbf{v}}(t)(\mathbf{Q} \oplus \mathbf{A}/T), \quad \text{with initial value } \tilde{\mathbf{v}}(0) = \mathbf{0}. \tag{38}$$

Using (27) and the fact that $(\mathbf{Q} \oplus \mathbf{A}/T)$ is a transient generator, $\tilde{\mathbf{v}}(t)$ converges to $\tilde{\mathbf{v}}(\infty) = \lim_{t\to\infty} \tilde{\mathbf{v}}(t) = -(\boldsymbol{\pi} \otimes \mathbf{I}_N)(\mathbf{Q} \oplus \mathbf{A}/T)^{-1}$. From which, we have

$$\mathbf{P}^*(-\mathbf{A}/T) = \int_{t=0}^{\infty} \mathbf{p}(t) \otimes e^{\mathbf{A}t/T}\mathrm{d}t = \int_{t=0}^{\infty} \mathbf{p}(t) \otimes \mathbf{u}(t)\mathrm{d}t = \int_{t=0}^{\infty} \mathbf{v}(t)\mathrm{d}t = \tilde{\mathbf{v}}(\infty),$$

which results in the theorem. □

Finally, for the NILT based transient analysis of CTMCs, we obtain

$$\begin{aligned} \boldsymbol{p}(T) \approx \boldsymbol{p}_N(T) &= (\mathbf{I}_1 \otimes \boldsymbol{\alpha})\mathbf{P}^*(-\mathbf{A}/T)(\mathbf{I}_S \otimes \boldsymbol{a}/T) \\ &= -(\boldsymbol{\pi} \otimes \boldsymbol{\alpha})(\mathbf{Q} \oplus \mathbf{A}/T)^{-1}(\mathbf{I}_S \otimes \boldsymbol{a}/T). \end{aligned} \tag{39}$$

4 Transient analysis of Markov fluid models

This section applies the same analysis steps for MFMs as Section 3 for CTMCs. Unfortunately, the analysis of MFMs is more complex than the analysis of CTMCs. To help the reader through this complex analysis, Section 3 and 4 are synchronized in their subsection structure and analytical discussion. That is, the goals of the subsections of Section 4 are the same as goals of the related subsections in Section 3.

First we state that the transient analysis of MFMs with NILT and with random clock are identical, and in consecutive subsections, we present the analysis details of the two approaches.

Theorem 5. *The transient fluid density and empty buffer probability of the MFM with initial probability vector* $\boldsymbol{\pi}$*, generator* $\mathbf{Q}$ *and fluid rate matrix* $\mathbf{R}$ *computed by the random clock method and by NILT are identical when the same MEWF,* $f_N(t) = \boldsymbol{\alpha} e^{\mathbf{A}t} \boldsymbol{a}$*, is used.*

Proof. In the following subsections, we show that the random clock based analysis results in (73) and (74), and the NILT based analysis results in (84) and (85), which are identical. □

4.1 Background

MFMs are $(X(t), Y(t))$ vector valued Markov processes, where $X(t) \in \mathcal{S} = \{1, 2, \ldots, S\}$ is a CTMC with generator $\mathbf{Q}$ and $Y(t) \in \mathbb{R}^+$ is referred to as fluid level. $Y(t)$ increases with r_i while $X(t) = i$ and $Y(t) > 0$. To keep the subsequent discussion reasonably simple, we apply the following assumptions:

- $Y(t)$ is not upper bounded (infinite buffer fluid model),
- $\Pr(X(0) = i) = \pi_i$,
- $Y(0) = 0$,
- $r_i \neq 0$,
- the states are numbered such that the first S_+ states have positive rates and the next S_- states have negative rates where $S = S_+ + S_-$. Accordingly, the block structure of the generator and the rate matrices are $\mathbf{Q} = \begin{array}{|c|c|}\hline \mathbf{Q}_+ & \mathbf{Q}_{+-} \\ \hline \mathbf{Q}_{-+} & \mathbf{Q}_- \\ \hline \end{array}$ and $\mathbf{R} = \begin{array}{|c|c|}\hline \mathbf{R}_+ & \\ \hline & \mathbf{R}_- \\ \hline \end{array}$.

The fluid density and empty buffer probability vectors, $\boldsymbol{p}(t, x)$ and $\boldsymbol{\ell}(t)$, whose jth elements are defined as

- $p_j(t,x) = \frac{\partial}{\partial x}\Pr(Y(t) < x, X(t) = j)$ for $j \in \mathcal{S}$, and
- $\ell_j(t) = \Pr(Y(t) = 0, X(t) = j)$ for $j \in \mathcal{S}_-$,

satisfy the following differential equations and initial conditions:

For $x > 0$,

$$\frac{\partial}{\partial t}\boldsymbol{p}(t,x) + \frac{\partial}{\partial x}\boldsymbol{p}(t,x)\mathbf{R} = \boldsymbol{p}(t,x)\mathbf{Q} \quad \text{with} \quad \boldsymbol{p}(0,x) = 0, \tag{40}$$

for $x = 0$ and $t > 0$

$$\boldsymbol{p}_+(t,0)\mathbf{R}_+ = \boldsymbol{\ell}(t)\mathbf{Q}_{-+} \quad \text{with} \quad \boldsymbol{p}_+(0,0) = \hat{\delta}\boldsymbol{\pi}_+\mathbf{R}_+^{-1}, \boldsymbol{\ell}(0) = \boldsymbol{\pi}_- \ , \tag{41}$$

and

$$\frac{d}{dt}\boldsymbol{\ell}(t) = \boldsymbol{\ell}(t)\mathbf{Q}_- - \boldsymbol{p}_-(t,0)\mathbf{R}_- \quad \text{with} \quad \boldsymbol{\ell}(0) = \boldsymbol{\pi}_-, \tag{42}$$

where $\hat{\delta}$ represents the Dirac impulse at zero. In contrast to the case of CTMCs, easy to compute numerical methods are not available for $\boldsymbol{p}(t,x)$ and $\boldsymbol{\ell}(t)$.

4.1.1 Laplace transform domain description

The LT domain description of the fluid density and the empty buffer probability vectors are $\boldsymbol{p}^*(s,x) = \int_{t=0}^{\infty} e^{-st}\boldsymbol{p}(t,x)dt$ and $\boldsymbol{\ell}^*(s) = \int_{t=0}^{\infty} e^{-st}\boldsymbol{\ell}(t)dt$. The analysis of these vectors is based on an essential measure, which is associated with the first visit to level zero. Let $\gamma = \min(t|Y(t) = 0, t > 0)$ be the first time when the fluid level decreases to zero. The return measure of interest is

$$\Psi_{ij}(t) = \Pr(\gamma < t, X(\gamma) = j | Y(0) = 0, X(0) = i),$$

where $i \in S_+$ and $j \in S_-$. The matrix formed of these elements is $\boldsymbol{\Psi}(t) = \{\Psi_{ij}(t)\}$ and its LT is $\boldsymbol{\Psi}^*(s) = \int_{t=0}^{\infty} e^{-st}\boldsymbol{\Psi}(t)dt$, which satisfies the non-symmetric algebraic Riccati equation (NARE) [8]

$$\mathbf{0} = \mathbf{Q}_+(s)\boldsymbol{\Psi}^*(s) + \boldsymbol{\Psi}^*(s)\mathbf{Q}_-(s) + \boldsymbol{\Psi}^*(s)\mathbf{Q}_{-+}(s)\boldsymbol{\Psi}^*(s) + \mathbf{Q}_{+-}(s), \tag{43}$$

with

$$\begin{aligned} \mathbf{Q}_+(s) &= \mathbf{R}_+^{-1}(\mathbf{Q}_+ - s\mathbf{I}) \ , \quad \mathbf{Q}_{+-}(s) = \mathbf{R}_+^{-1}\mathbf{Q}_{+-} \ , \\ \mathbf{Q}_{-+}(s) &= -\mathbf{R}_-^{-1}\mathbf{Q}_{-+} \ , \quad \mathbf{Q}_-(s) = -\mathbf{R}_-^{-1}(\mathbf{Q}_- - s\mathbf{I}) \ . \end{aligned}$$

There are efficient numerical solution methods to compute $\mathbf{\Psi}^*(s)$ based on (43) [7]. Having computed $\mathbf{\Psi}^*(s)$, the matrix characterizing the fluid increase is obtained as [4]

$$\mathbf{K}^*(s) = \mathbf{Q}_+(s) + \mathbf{\Psi}^*(s)\mathbf{Q}_{-+}(s). \tag{44}$$

When the initial probability vector is $\boldsymbol{\pi} = [\boldsymbol{\pi}_+, \boldsymbol{\pi}_-]$ and the initial fluid level is zero, the LTs are given by [3]

$$\boldsymbol{\ell}^*(s) = \left(\boldsymbol{\pi}_+\mathbf{\Psi}^*(s) + \boldsymbol{\pi}_-\right)\left(s\mathbf{I} - \mathbf{Q}_- - \mathbf{Q}_{-+}\mathbf{\Psi}^*(s)\right)^{-1}, \tag{45}$$

$$\boldsymbol{p}^*(s,x) = \left(\boldsymbol{\pi}_+ + \boldsymbol{\ell}^*(s)\mathbf{Q}_{-+}\right)e^{\mathbf{K}^*(s)x}\left[\mathbf{R}_+^{-1}, -\mathbf{\Psi}^*(s)\mathbf{R}_-^{-1}\right]. \tag{46}$$

4.1.2 Stationary distribution

When $\mathbf{Q}$ is an irreducible generator with stationary distribution satisfying $\boldsymbol{p}\mathbf{Q} = \mathbf{0}$, and $\boldsymbol{p}\mathbb{1} = 1$, and $\boldsymbol{p}\mathbf{R}\mathbb{1} < 0$, then the stationary distribution of this MFM, $\boldsymbol{p}(x) = \lim_{t\to\infty}\boldsymbol{p}(t,x)$ and $\boldsymbol{\ell} = \lim_{t\to\infty}\boldsymbol{\ell}(t)$, is obtained as follows [14]. The stationary distribution, $\boldsymbol{\ell}$, is the solution of the linear system

$$\boldsymbol{\ell}\left(\mathbf{Q}_- + \mathbf{Q}_{-+}\mathbf{\Psi}\right) = \mathbf{0}, \quad \boldsymbol{\ell}\mathbb{1} + \boldsymbol{\ell}\mathbf{Q}_{-+}\left(-\mathbf{K}\right)^{-1}\left[\mathbf{R}_+^{-1}, -\mathbf{\Psi}\mathbf{R}_-^{-1}\right]\mathbb{1} = 1, \tag{47}$$

and

$$\boldsymbol{p}(x) = \boldsymbol{\ell}e^{\mathbf{K}x}\left[\mathbf{R}_+^{-1}, -\mathbf{\Psi}\mathbf{R}_-^{-1}\right], \tag{48}$$

where $\mathbf{\Psi} = \mathbf{\Psi}^*(s)|_{s=0}$ and $\mathbf{K} = \mathbf{K}^*(s)|_{s=0}$.

In the special case, where the generator of the modulating Markov chain is $\mathbf{Q}^0$ (instead of $\mathbf{Q}$) when the buffer is empty, (40) remains valid, but instead of (41) and (42) we have

$$\begin{aligned}\boldsymbol{p}_+(t,0)\mathbf{R}_+ &= \boldsymbol{\ell}(t)\mathbf{Q}_{-+}^0 \quad \text{with} \quad \boldsymbol{p}_+(0,0) = \delta(0)\boldsymbol{\pi}_+\mathbf{R}_+^{-1}, \text{ and}\\ \frac{d}{dt}\boldsymbol{\ell}(t) &= \boldsymbol{\ell}(t)\mathbf{Q}_-^0 - \boldsymbol{p}_-(t,0)\mathbf{R}_- \quad \text{with} \quad \boldsymbol{\ell}(0) = \boldsymbol{\pi}_-,\end{aligned}$$

from which the stationary empty buffer distribution, vector $\boldsymbol{\ell}$, is obtained as the solution of the linear system

$$\boldsymbol{\ell}\left(\mathbf{Q}_-^0 + \mathbf{Q}_{-+}^0\mathbf{\Psi}\right) = \mathbf{0}, \quad \boldsymbol{\ell}\mathbb{1} + \boldsymbol{\ell}\mathbf{Q}_{-+}^0\left(-\mathbf{K}\right)^{-1}\left[\mathbf{R}_+^{-1}, -\mathbf{\Psi}\mathbf{R}_-^{-1}\right]\mathbb{1} = 1. \tag{49}$$

The stationary fluid density, $\boldsymbol{p}(x)$, can be computed from (48) using this vector $\boldsymbol{\ell}$.

4.1.3 Transient Markov fluid model

When $\mathbf{Q}$ is a transient generator whose eigenvalues have strictly negative real parts, then $\lim_{t\to\infty} \boldsymbol{p}(t,x) = \mathbf{0}$ and $\lim_{t\to\infty} \boldsymbol{\ell}(t) = \mathbf{0}$. In this case, we are interested in $\tilde{\boldsymbol{p}}(t,x) = \int_{\tau=0}^{t} \boldsymbol{p}(\tau,x)\mathrm{d}\tau$ and $\tilde{\boldsymbol{\ell}}(t) = \int_{\tau=0}^{t} \boldsymbol{\ell}(t)\mathrm{d}\tau$. Integrating (40)-(42) from 0 to t gives

$$\begin{aligned}
\frac{\partial}{\partial t}\tilde{\boldsymbol{p}}(t,x) + \frac{\partial}{\partial x}\tilde{\boldsymbol{p}}(t,x)\mathbf{R} &= \tilde{\boldsymbol{p}}(t,x)\mathbf{Q} \quad \text{with} \quad \tilde{\boldsymbol{p}}(0,x) = 0, \\
\tilde{\boldsymbol{p}}_+(t,0)\mathbf{R}_+ &= \boldsymbol{\pi}_+ + \tilde{\boldsymbol{\ell}}(t)\mathbf{Q}_{-+}, \\
\frac{d}{dt}\tilde{\boldsymbol{\ell}}(t) - \boldsymbol{\pi}_- &= \tilde{\boldsymbol{\ell}}(t)\mathbf{Q}_- - \tilde{\boldsymbol{p}}_-(t,0)\mathbf{R}_- \quad \text{with} \quad \tilde{\boldsymbol{\ell}}(0) = \mathbf{0},
\end{aligned}$$

where we used $\int_{0^-}^{t} \boldsymbol{p}_+(\tau,0)\mathbf{R}_+\mathrm{d}\tau = \int_{0^-}^{0^+} \boldsymbol{p}_+(\tau,0)\mathbf{R}_+\mathrm{d}\tau + \int_{0^+}^{t} \boldsymbol{p}_+(\tau,0)\mathbf{R}_+\mathrm{d}\tau = \boldsymbol{\pi}_+ + \int_{0^+}^{t} \boldsymbol{\ell}(\tau)\mathbf{Q}_{-+}\mathrm{d}\tau$ in the second equation.

For the stationary limits $\tilde{\boldsymbol{p}}(\infty,x) = \lim_{t\to\infty} \tilde{\boldsymbol{p}}(t,x)$ and $\tilde{\boldsymbol{\ell}}(\infty) = \lim_{t\to\infty} \tilde{\boldsymbol{\ell}}(t)$, the characterizing equations can be decomposed to the following matrix block equations

$$\frac{d}{dx}\tilde{\boldsymbol{p}}_+(\infty,x)\mathbf{R}_+ = \tilde{\boldsymbol{p}}_+(\infty,x)\mathbf{Q}_+ + \tilde{\boldsymbol{p}}_-(\infty,x)\mathbf{Q}_{-+}, \tag{50}$$

$$\frac{d}{dx}\tilde{\boldsymbol{p}}_-(\infty,x)\mathbf{R}_- = \tilde{\boldsymbol{p}}_-(\infty,x)\mathbf{Q}_- + \tilde{\boldsymbol{p}}_+(\infty,x)\mathbf{Q}_{+-}, \tag{51}$$

$$\tilde{\boldsymbol{p}}_+(\infty,0)\mathbf{R}_+ - \boldsymbol{\pi}_+ = \tilde{\boldsymbol{\ell}}(\infty)\mathbf{Q}_{-+}, \tag{52}$$

$$-\boldsymbol{\pi}_- = \tilde{\boldsymbol{\ell}}(\infty)\mathbf{Q}_- - \tilde{\boldsymbol{p}}_-(\infty,0)\mathbf{R}_-. \tag{53}$$

Theorem 6. *The solution of* (50) - (53) *is*

$$\tilde{\boldsymbol{\ell}}(\infty) = -\left(\boldsymbol{\pi}_+\boldsymbol{\Psi} + \boldsymbol{\pi}_-\right)\left(\mathbf{Q}_- + \mathbf{Q}_{-+}\boldsymbol{\Psi}\right)^{-1}, \tag{54}$$

$$\tilde{\boldsymbol{p}}_+(\infty,x) = (\boldsymbol{\pi}_+ + \tilde{\boldsymbol{\ell}}(\infty)\mathbf{Q}_{-+})e^{\mathbf{K}x}\mathbf{R}_+^{-1}, \tag{55}$$

$$\tilde{\boldsymbol{p}}_-(\infty,x) = -(\boldsymbol{\pi}_+ + \tilde{\boldsymbol{\ell}}(\infty)\mathbf{Q}_{-+})e^{\mathbf{K}x}\boldsymbol{\Psi}\mathbf{R}_-^{-1}, \tag{56}$$

where $\boldsymbol{\Psi}$ *is the solution of*

$$\mathbf{0} = \mathbf{R}_+^{-1}\mathbf{Q}_+\boldsymbol{\Psi} - \boldsymbol{\Psi}\mathbf{R}_-^{-1}\mathbf{Q}_- - \boldsymbol{\Psi}\mathbf{R}_-^{-1}\mathbf{Q}_{-+}\boldsymbol{\Psi} + \mathbf{R}_+^{-1}\mathbf{Q}_{+-}, \tag{57}$$

and

$$\mathbf{K} = \mathbf{R}_+^{-1}\mathbf{Q}_+ - \boldsymbol{\Psi}\mathbf{R}_-^{-1}\mathbf{Q}_{-+}. \tag{58}$$

Proof. Substituting $\tilde{\boldsymbol{\ell}}(\infty)$, $\tilde{\boldsymbol{p}}_+(\infty,x)$ and $\tilde{\boldsymbol{p}}_-(\infty,x)$ into (50) - (53) gives the statements of the theorem. □

While (27) is a widely known result, Theorem 6 is new according to the author's latest knowledge. Furthermore, the structural similarity of (45)-(46) and (54)-(56) and the fact that $\mathbf{Q} - s\mathbf{I}$ is a transient generator for $s > 0$ suggest that the analysis of transient processes and the LT domain description of the same processes are closely related, but this relation is not investigated in the current work.

4.2 Markov fluid model augmented with a random clock

Similar to the case of CTMC, we augment an MFM characterized by the initial probability vector $\boldsymbol{\pi}$, the generator matrix $\mathbf{Q}$ and the fluid rate matrix $\mathbf{R}$, with a random clock whose weight function, $f_N(t/T)/T = \boldsymbol{\alpha} e^{\mathbf{A}t/T}\boldsymbol{a}/T$, is normalized and centralized at T [5]. The state space of the MFM augmented with a random clock has a block of size SN, which describes the parallel evolution of the original MFM and the clock; and a block of size one, which is used for resetting the model after a clock event.

We need the following definitions for the steady-state distribution of the clock augmented MFM of size $SN + 1$, $(\hat{X}(t), \hat{Y}(t))$. Let $\hat{\boldsymbol{\ell}}$ and $\hat{\mathbf{p}}(x)$ be the steady-state fluid density and the empty buffer probability vectors of the extended MFM $(\hat{X}(t), \hat{Y}(t))$, whose jth elements are

$$\hat{p}_j(x) = \lim_{t\to\infty} \frac{d}{dx} \Pr(\hat{Y}(t) \le x, \hat{X}(t) = j), \text{ for } x \ge 0, \tag{59}$$

$$\hat{\ell}_j = \lim_{t\to\infty} \Pr(\hat{Y}(t) = 0, \hat{X}(t) = j). \tag{60}$$

The extended model is such that, the original MFM and the clock evolves parallel until a clock event. At a clock event, the process moves to state $SN + 1$ and a reset process starts, during which the fluid level decreases to zero at rate -1. After reaching fluid level zero in state $SN+1$ an exponential transition takes place at rate one to the initial state of the next cycle. Since the performance measure of our interest is the behaviour of the augmented MFM at clock events, the rate at which the fluid level decreases to zero and the parameter of the exponentially distributed time spent in the reset state do not play roles.

At the end of the reset process, the original CTMC is set to state j with probability π_j, the fluid level is 0, and the state vector of the clock is reset to its initial state, $\boldsymbol{\alpha}$. After a reset, the parallel evolution of the original model and the clock and the reset phase repeat in consecutive cycles.

Fig. 1 demonstrates the evolution of the MFM augmented with a random clock. The extended MFM, $(\hat{X}(t), \hat{Y}(t))$, follows a cyclic behaviour of

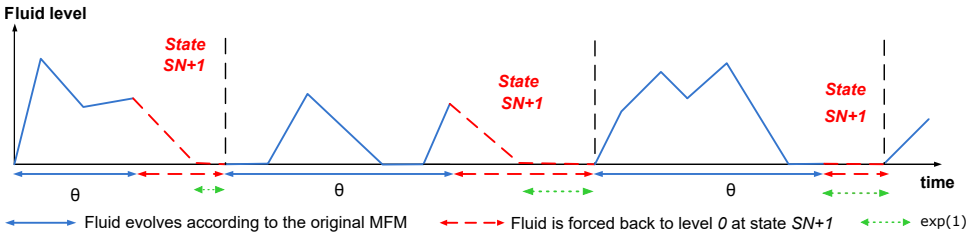

Figure 1: A sample path of the fluid level process of the extended MFM

stochastically identical cycles (separated by vertical dashed lines in Fig. 1). In each cycle, the extended MFM starts from level 0 and with initial probability vector $\boldsymbol{\pi}$ and spends an $f_N(t/T)/T$ distributed time (denoted by θ in the figure) in the subset of the first SN states. In the figure, cycle 1 and 3 starts with a positive rate, cycle 2 starts with a negative rate, and in cycle 1 and 2 the clock expires at a positive fluid level, while in cycle 3 it expires when the fluid level is zero.

Unfortunately, to empty the fluid buffer for the end of the reset phase the extended MFM has a fluid level dependent behaviour, which means that the extended model is governed by different generator and rate matrix when the fluid level is positive, $\hat{\mathbf{Q}}$ and $\hat{\mathbf{R}}$, and when the buffer is empty, $\hat{\mathbf{Q}}^0$ and $\hat{\mathbf{R}}^0$. The block structure of these matrices are

$$\hat{\mathbf{Q}} = \begin{array}{c|cc} & SN & 1 \\ \hline SN & \bar{\mathbf{Q}} & \mathbb{1} \otimes \boldsymbol{a}/T \\ 1 & \mathbf{0} & 0 \end{array} = \begin{array}{c|cc} & SN & 1 \\ \hline SN & \mathbf{Q} \oplus \mathbf{A}/T & \mathbb{1} \otimes \boldsymbol{a}/T \\ 1 & \mathbf{0} & 0 \end{array}, \quad \hat{\mathbf{R}} = \begin{array}{c|cc} & SN & 1 \\ \hline SN & \bar{\mathbf{R}} & \mathbf{0} \\ 1 & \mathbf{0} & -1 \end{array} = \begin{array}{c|cc} & SN & 1 \\ \hline SN & \mathbf{R} \otimes \mathbf{I} & \mathbf{0} \\ 1 & \mathbf{0} & -1 \end{array},$$

$$\hat{\mathbf{Q}}^0 = \begin{array}{|c|c|} \hline \bar{\mathbf{Q}} & \mathbb{1} \otimes \boldsymbol{a}/T \\ \hline \boldsymbol{\pi} \otimes \boldsymbol{\alpha} & -1 \\ \hline \end{array} = \begin{array}{|c|c|} \hline \mathbf{Q} \oplus \mathbf{A}/T & \mathbb{1} \otimes \boldsymbol{a}/T \\ \hline \boldsymbol{\pi} \otimes \boldsymbol{\alpha} & -1 \\ \hline \end{array}, \quad \hat{\mathbf{R}}^0 = \begin{array}{|c|c|} \hline \bar{\mathbf{R}} & \mathbf{0} \\ \hline \mathbf{0} & -1 \\ \hline \end{array} = \begin{array}{|c|c|} \hline \mathbf{R} \otimes \mathbf{I} & \mathbf{0} \\ \hline \mathbf{0} & -1 \\ \hline \end{array},$$

where the numbers outside the blocks indicate the dimension of the matrix blocks considering that the diagonal blocks are square matrices.

The number of states with positive rate is S_+N and the number of states with negative rate is $S_-N + 1$. Based on the sign of the fluid rates of the original MFM, we can decompose matrix $\bar{\mathbf{Q}} = \mathbf{Q} \oplus \mathbf{A}/T$ into the following blocks

$$\mathbf{Q} \oplus \mathbf{A}/T = \mathbf{Q} \otimes \mathbf{I}_N + \mathbf{I}_S \otimes \mathbf{A}/T = \begin{array}{|c|c|} \hline \mathbf{Q}_+ \oplus \mathbf{A}/T & \mathbf{Q}_{+-} \otimes \mathbf{I}_N \\ \hline \mathbf{Q}_{-+} \otimes \mathbf{I}_N & \mathbf{Q}_- \oplus \mathbf{A}/T \\ \hline \end{array},$$

where the subscripts of the identity matrices indicate their size, e.g., $\mathbf{I}_S$ is of size S.

The fluid rate dependent block structure of $\hat{\mathbf{Q}}$, $\hat{\mathbf{R}}$, $\hat{\mathbf{Q}}^0$ and $\hat{\mathbf{R}}^0$ are

$$\hat{\mathbf{Q}} = \begin{array}{c|c} \bar{\mathbf{Q}} & \mathbb{1} \otimes \boldsymbol{a}/T \\ \hline \mathbf{0} & 0 \end{array} = \begin{array}{c|c|c} \mathbf{Q}_+ \oplus \mathbf{A}/T & \mathbf{Q}_{+-} \otimes \mathbf{I}_N & \mathbb{1}_+ \otimes \boldsymbol{a}/T \\ \hline \mathbf{Q}_{-+} \otimes \mathbf{I}_N & \mathbf{Q}_- \oplus \mathbf{A}/T & \mathbb{1}_- \otimes \boldsymbol{a}/T \\ \hline \mathbf{0} & \mathbf{0} & 0 \end{array} = \begin{array}{c|c} \hat{\mathbf{Q}}_+ & \hat{\mathbf{Q}}_{+-} \\ \hline \hat{\mathbf{Q}}_{-+} & \hat{\mathbf{Q}}_- \end{array},$$

$$\hat{\mathbf{Q}}^0 = \begin{array}{c|c} \bar{\mathbf{Q}} & \mathbb{1} \otimes \boldsymbol{a}/T \\ \hline \boldsymbol{\pi} \otimes \boldsymbol{\alpha} & -1 \end{array} = \begin{array}{c|c|c} \mathbf{Q}_+ \oplus \mathbf{A}/T & \mathbf{Q}_{+-} \otimes \mathbf{I}_N & \mathbb{1}_+ \otimes \boldsymbol{a}/T \\ \hline \mathbf{Q}_{-+} \otimes \mathbf{I}_N & \mathbf{Q}_- \oplus \mathbf{A}/T & \mathbb{1}_- \otimes \boldsymbol{a}/T \\ \hline \boldsymbol{\pi}_+ \otimes \boldsymbol{\alpha} & \boldsymbol{\pi}_- \otimes \boldsymbol{\alpha} & -1 \end{array} = \begin{array}{c|c} \hat{\mathbf{Q}}^0_+ & \hat{\mathbf{Q}}^0_{+-} \\ \hline \hat{\mathbf{Q}}^0_{-+} & \hat{\mathbf{Q}}^0_- \end{array},$$

$$\hat{\mathbf{R}} = \hat{\mathbf{R}}^0 = \begin{array}{c|c} \bar{\mathbf{R}} & \mathbf{0} \\ \hline \mathbf{0} & -1 \end{array} = \begin{array}{c|c|c} \mathbf{R}_+ \otimes \mathbf{I} & \mathbf{0} & \mathbf{0} \\ \hline \mathbf{0} & \mathbf{R}_- \otimes \mathbf{I} & \mathbf{0} \\ \hline \mathbf{0} & \mathbf{0} & -1 \end{array} = \begin{array}{c|c} \hat{\mathbf{R}}_+ & \\ \hline & \hat{\mathbf{R}}_- \end{array}.$$

Based on this partitioning of the extended state space, we partition vectors $\hat{\boldsymbol{\ell}}$ and $\hat{\mathbf{p}}(x)$ as follows

$$\underbrace{\hat{\boldsymbol{\ell}}}_{S_-\times N+1} = [\underbrace{\bar{\boldsymbol{\ell}}}_{S_-\times N}, \underbrace{\ell^{\triangle}}_{1}], \tag{61}$$

$$\underbrace{\hat{\mathbf{p}}(x)}_{S\times N+1} = [\underbrace{\hat{\mathbf{p}}_+(x)}_{S_+\times N}, \underbrace{\hat{\mathbf{p}}_-(x)}_{S_-\times N+1}] = [\underbrace{\bar{\mathbf{p}}(x)}_{S\times N}, \underbrace{p^{\triangle}(x)}_{1}] = [\underbrace{\bar{\mathbf{p}}_+(x)}_{S_+\times N}, \underbrace{\bar{\mathbf{p}}_-(x)}_{S_-\times N}, \underbrace{p^{\triangle}(x)}_{1}] \tag{62}$$

According to Section 4.1.2, the stationary distribution of such fluid level dependent MFM is $\hat{\boldsymbol{\ell}}$ and $\hat{\mathbf{p}}(x)$, where $\hat{\boldsymbol{\ell}}$ is the solution of the linear system

$$\hat{\boldsymbol{\ell}}\left(\hat{\mathbf{Q}}^0_- + \hat{\mathbf{Q}}^0_{-+}\hat{\boldsymbol{\Psi}}\right) = \mathbf{0}, \tag{63}$$

$$\hat{\boldsymbol{\ell}}\mathbb{1} + \hat{\boldsymbol{\ell}}\hat{\mathbf{Q}}^0_{-+}\left(-\hat{\mathbf{K}}\right)^{-1}\left[\hat{\mathbf{R}}_+^{-1}, -\hat{\boldsymbol{\Psi}}\hat{\mathbf{R}}_-^{-1}\right]\mathbb{1} = 1, \tag{64}$$

and

$$\hat{\mathbf{p}}(x) = \hat{\boldsymbol{\ell}}\hat{\mathbf{Q}}^0_{-+}e^{\hat{\mathbf{K}}x}\left[\hat{\mathbf{R}}_+^{-1}, -\hat{\boldsymbol{\Psi}}\hat{\mathbf{R}}_-^{-1}\right]. \tag{65}$$

Matrices $\hat{\boldsymbol{\Psi}}$ and $\hat{\mathbf{K}}$ are obtained from $\hat{\mathbf{Q}}$ and $\hat{\mathbf{R}}$ in the same way as $\boldsymbol{\Psi}$ and $\mathbf{K}$ are obtained from $\mathbf{Q}$ and $\mathbf{R}$. That is,

$$\mathbf{0} = \hat{\mathbf{R}}_+^{-1}\hat{\mathbf{Q}}_+\hat{\boldsymbol{\Psi}} - \hat{\boldsymbol{\Psi}}\hat{\mathbf{R}}_-^{-1}\hat{\mathbf{Q}}_- - \hat{\boldsymbol{\Psi}}\hat{\mathbf{R}}_-^{-1}\hat{\mathbf{Q}}_{-+}\hat{\boldsymbol{\Psi}} + \hat{\mathbf{R}}_+^{-1}\hat{\mathbf{Q}}_{+-}, \tag{66}$$

$$\hat{\mathbf{K}} = \hat{\mathbf{R}}_+^{-1}\hat{\mathbf{Q}}_+ - \hat{\boldsymbol{\Psi}}\hat{\mathbf{R}}_-^{-1}\hat{\mathbf{Q}}_{-+}. \tag{67}$$

The size SN part of the stationary solution of the size $SN+1$ extended model is easily computed for CTMCs in (29). The following lemma provides the related relations for MFMs.

Lemma 1. *Let* $\bar{\mathbf{\Psi}}$ *and* $\bar{\mathbf{K}}$ *be obtained from*

$$\mathbf{0} = \bar{\mathbf{R}}_+^{-1}\bar{\mathbf{Q}}_+\bar{\mathbf{\Psi}} - \bar{\mathbf{\Psi}}\bar{\mathbf{R}}_-^{-1}\bar{\mathbf{Q}}_- - \bar{\mathbf{\Psi}}\bar{\mathbf{R}}_-^{-1}\bar{\mathbf{Q}}_{-+}\bar{\mathbf{\Psi}} + \bar{\mathbf{R}}_+^{-1}\bar{\mathbf{Q}}_{+-}, \tag{68}$$

$$\bar{\mathbf{K}} = \bar{\mathbf{R}}_+^{-1}\bar{\mathbf{Q}}_+ - \bar{\mathbf{\Psi}}\bar{\mathbf{R}}_-^{-1}\bar{\mathbf{Q}}_{-+}, \tag{69}$$

then $\hat{\mathbf{\Psi}} = \left[\bar{\mathbf{\Psi}}, \Psi^{\triangle}\right]$ *and* $\hat{\mathbf{K}} = \bar{\mathbf{K}}$*, where* $\Psi^{\triangle}$ *is of size* $S_+N \times 1$*.*

Proof. Decomposing (66) and (67) according to the block structure of $\hat{\mathbf{Q}}$ and $\hat{\mathbf{R}}$ results in the lemma. □

Using the decomposition of matrices $\hat{\mathbf{Q}}^0$ and $\hat{\mathbf{\Psi}}$ and vector $\hat{\boldsymbol{\ell}}$, (63) can be written as

$$\begin{aligned}\mathbf{0} &= \hat{\boldsymbol{\ell}}\left(\hat{\mathbf{Q}}_-^0 + \hat{\mathbf{Q}}_{-+}^0\hat{\mathbf{\Psi}}\right)\\ &= [\bar{\boldsymbol{\ell}}, \ell^{\triangle}]\left(\begin{array}{|c|c|}\hline \mathbf{Q}_- \oplus \mathbf{A}/T & \mathbb{1}_- \otimes \boldsymbol{a}/T \\ \hline \boldsymbol{\pi}_- \otimes \boldsymbol{\alpha} & -1 \\ \hline\end{array} + \begin{array}{|c|c|}\hline (\mathbf{Q}_{-+} \otimes \mathbf{I}_N)\bar{\mathbf{\Psi}} & (\mathbf{Q}_{-+} \otimes \mathbf{I}_N)\Psi^{\triangle} \\ \hline (\boldsymbol{\pi}_+ \otimes \boldsymbol{\alpha})\bar{\mathbf{\Psi}} & (\boldsymbol{\pi}_+ \otimes \boldsymbol{\alpha})\Psi^{\triangle} \\ \hline\end{array}\right),\end{aligned}$$

from which

$$\bar{\boldsymbol{\ell}} = \ell^{\triangle}\underbrace{\left(-(\boldsymbol{\pi}_- \otimes \boldsymbol{\alpha}) - (\boldsymbol{\pi}_+ \otimes \boldsymbol{\alpha})\bar{\mathbf{\Psi}}\right)\left((\mathbf{Q}_- \oplus \mathbf{A}/T) + (\mathbf{Q}_{-+} \otimes \mathbf{I}_N)\bar{\mathbf{\Psi}}\right)^{-1}}_{\stackrel{\text{def}}{=}\ \vec{\boldsymbol{\ell}}} = \ell^{\triangle}\vec{\boldsymbol{\ell}}. \tag{70}$$

Also in this case, $(\mathbf{Q}_- \oplus \mathbf{A}/T) + (\mathbf{Q}_{-+} \otimes \mathbf{I}_N)\bar{\mathbf{\Psi}}$ is non-singular, when the eigenvalues of $\mathbf{A}$ have negative real parts.

Based on (65), (70) and the $\hat{\mathbf{\Psi}} = \boxed{\bar{\mathbf{\Psi}}\,|\,\Psi^{\triangle}}$ decomposition of $\hat{\mathbf{\Psi}}$, we have

$$\bar{\boldsymbol{p}}(x) = \hat{\boldsymbol{\ell}}\hat{\mathbf{Q}}_{-+}^0 e^{\hat{\mathbf{K}}x}\left[\hat{\mathbf{R}}_+^{-1}, -\bar{\mathbf{\Psi}}\left(\mathbf{R}_-^{-1} \otimes \mathbf{I}_N\right)\right] \tag{71}$$

$$\begin{aligned}&= [\bar{\boldsymbol{\ell}}, \ell^{\triangle}]\boxed{\begin{array}{c}\mathbf{Q}_{-+} \otimes \mathbf{I}_N \\ \hline \boldsymbol{\pi}_+ \otimes \boldsymbol{\alpha}\end{array}} e^{\hat{\mathbf{K}}x}\left[\left(\mathbf{R}_+^{-1} \otimes \mathbf{I}_N\right), -\bar{\mathbf{\Psi}}\left(\mathbf{R}_-^{-1} \otimes \mathbf{I}_N\right)\right]\\ &= \ell^{\triangle}\underbrace{\left(\vec{\boldsymbol{\ell}}(\mathbf{Q}_{-+} \otimes \mathbf{I}_N) + (\boldsymbol{\pi}_+ \otimes \boldsymbol{\alpha})\right)}_{\stackrel{\text{def}}{=}\ \vec{\vec{\boldsymbol{\ell}}}} e^{\hat{\mathbf{K}}x}\underbrace{\left[\left(\mathbf{R}_+^{-1} \otimes \mathbf{I}_N\right), -\bar{\mathbf{\Psi}}\left(\mathbf{R}_-^{-1} \otimes \mathbf{I}_N\right)\right]}_{\stackrel{\text{def}}{=}\ \vec{\vec{\mathbf{R}}}}\\ &= \ell^{\triangle}\vec{\vec{\boldsymbol{\ell}}}\ e^{\hat{\mathbf{K}}x}\vec{\vec{\mathbf{R}}}.\end{aligned} \tag{72}$$

For CTMCs, the normalizing condition was easily computer based on (32). The normalizing condition of MFMs is more complex, that is why we introduce the normalizing constant C in the following results.

Theorem 7. *The stationary embedded fluid density and empty buffer probability, $p_j^{(N)}(x)$ and $\ell_j^{(N)}$, at a clock event are obtained from the related stationary density and probability mass of $(\hat{X}(t), \hat{Y}(t))$ as*

$$\boldsymbol{\ell}^{(N)} = C\vec{\boldsymbol{\ell}}\left(\mathbf{I}_{S_-} \otimes \boldsymbol{a}/T\right), \tag{73}$$

$$\boldsymbol{p}^{(N)}(x) = C\overrightarrow{\boldsymbol{\ell}}\; e^{\hat{\mathbf{K}}x}\overrightarrow{\mathbf{R}}\left(\mathbf{I}_S \otimes \boldsymbol{a}/T\right), \tag{74}$$

where C is a normalizing constant.

Proof. This theorem is a counterpart of Theorem 3 and its proof follows a similar pattern. For $\ell_j^{(N)}$, we have

$$\ell_j^{(N)} = \lim_{\delta\to 0}\lim_{t\to\infty} \frac{\sum_{n=1}^{N} \Pr(\text{transition to } SN{+}1 \text{ in } (t,t{+}\delta), \hat{Y}(t)=0, \hat{X}(t)=(j,n))}{\Pr(\text{transition to } SN{+}1 \text{ in } (t,t{+}\delta))}$$

$$= \lim_{\delta\to 0}\lim_{t\to\infty} \frac{\displaystyle\sum_{n=1}^{N} \Pr(\text{transition to } SN{+}1 \text{ in } (t,t{+}\delta), \hat{Y}(t)=0, \hat{X}(t)=(j,n))}{\displaystyle\sum_{k=1}^{S}\sum_{n=1}^{N}\left(\int_{y=0}^{\infty} \Pr(\text{tr. to } SN{+}1 \text{ in } (t,t{+}\delta), \hat{Y}(t)=y, \hat{X}(t)=(k,n))dy \right.}$$
$$\left. + \Pr(\text{tr. to } SN{+}1 \text{ in } (t,t{+}\delta), \hat{Y}(t)=0, \hat{X}(t)=(k,n))\right).$$

When $\hat{X}(t)=(j,n)$, the probability that the $(\hat{X}(t), \hat{Y}(t))$ process moves to state $SN{+}1$ in $(t,t{+}\delta)$ is $(\delta a_n/T + \sigma(\delta))$. Using this infinitesimal behaviour, the last expression can be rewritten as

$$\ell_j^{(N)} = \lim_{\delta\to 0} \frac{\sum_{n=1}^{N} \hat{\ell}_{(j,n)}\left(\delta a_n/T + \sigma(\delta)\right)}{\sum_{k=1}^{S}\sum_{n=1}^{N}\left(\int_{y=0}^{\infty}\hat{p}_{(k,n)}(y)dy + \hat{\ell}_{(k,n)}\right)\left(\delta a_n/T + \sigma(\delta)\right)}$$

$$= \frac{\sum_{n=1}^{N} \hat{\ell}_{(j,n)} a_n/T}{\sum_{k=1}^{S}\sum_{n=1}^{N}\left(\int_{y=0}^{\infty}\hat{p}_{(k,n)}(y)dy + \hat{\ell}_{(k,n)}\right) a_n/T}. \tag{75}$$

The proof of (74) follows a similar pattern. The only difference is that the $p_j^{(N)}(x)$ density value is transformed to the probability of being in a small

environment of x, as follows

$$
\begin{aligned}
&p_j^{(N)}(x)\Delta + \sigma(\Delta) = \\
&\Pr(\text{the fluid level is in } (x, x{+}\Delta) \text{ and the MFM state is } j \text{ at a tr. to } SN{+}1) \\
&= \lim_{\delta\to 0}\lim_{t\to\infty} \frac{\Pr(\text{the fluid level is in } (x, x{+}\Delta) \text{ and the MFM state is } j \\ \qquad\qquad \text{at time } t \text{ and transition to } SN{+}1 \text{ in } (t, t{+}\delta))}{\Pr(\text{transition to } SN{+}1 \text{ in } (t, t{+}\delta))} \\
&= \lim_{\delta\to 0} \frac{\sum_{n=1}^{N} \left(\hat{p}_{(j,n)}(x)\Delta + \sigma(\Delta)\right)(\delta a_n/T + \sigma(\delta))}{\sum_{k=1}^{S}\sum_{n=1}^{N} \left(\int_{y=0}^{\infty} \hat{p}_{(k,n)}(y)dy + \hat{\ell}_{(k,n)}\right)(\delta a_n/T + \sigma(\delta))} \\
&= \frac{\sum_{n=1}^{N} \left(\hat{p}_{(j,n)}(x)\Delta + \sigma(\Delta)\right) a_n/T}{\sum_{k=1}^{S}\sum_{n=1}^{N} \left(\int_{y=0}^{\infty} \hat{p}_{(k,n)}(y)dy + \hat{\ell}_{(k,n)}\right) a_n/T}. \qquad (76)
\end{aligned}
$$

Dividing (76) by Δ and taking the limit $\Delta \to 0$ results in

$$
p_j^{(N)}(x) = \frac{\sum_{n=1}^{N} \hat{p}_{(j,n)}(x) a_n/T}{\sum_{k=1}^{S}\sum_{n=1}^{N} \left(\int_{y=0}^{\infty} \hat{p}_{(k,n)}(y)dy + \hat{\ell}_{(k,n)}\right) a_n/T}. \qquad (77)
$$

The vector form of (75) and (77) are

$$
\boldsymbol{\ell}^{(N)} = \frac{\bar{\boldsymbol{\ell}}\left(\mathbf{I}_{S_-} \otimes \boldsymbol{a}/T\right)}{\bar{\boldsymbol{\ell}}\left(\mathbb{1}_{S_-} \otimes \boldsymbol{a}/T\right) + \int_{y=0}^{\infty} \bar{\boldsymbol{p}}(y)dy\,(\mathbb{1}_N \otimes \boldsymbol{a}/T)}, \qquad (78)
$$

$$
\boldsymbol{p}^{(N)}(x) = \frac{\bar{\boldsymbol{p}}(x)\,(\mathbf{I}_S \otimes \boldsymbol{a}/T)}{\bar{\boldsymbol{\ell}}\left(\mathbb{1}_{S_-} \otimes \boldsymbol{a}/T\right) + \int_{y=0}^{\infty} \bar{\boldsymbol{p}}(y)dy\,(\mathbb{1}_N \otimes \boldsymbol{a}/T)}. \qquad (79)
$$

Substituting (70) and (71) into these expressions give

$$
\boldsymbol{\ell}^{(N)} = \frac{\ell^{\triangle}\vec{\boldsymbol{\ell}}\left(\mathbf{I}_{S_-} \otimes \boldsymbol{a}/T\right)}{\ell^{\triangle}\vec{\boldsymbol{\ell}}\left(\mathbb{1}_{S_-} \otimes \boldsymbol{a}/T\right) + \int_{y=0}^{\infty} \ell^{\triangle}\vec{\boldsymbol{\ell}}\; e^{\hat{\mathbf{K}}y}\vec{\mathbf{R}}dy\,(\mathbb{1}_N \otimes \boldsymbol{a}/T)}, \qquad (80)
$$

$$
\boldsymbol{p}^{(N)}(x) = \frac{\ell^{\triangle}\vec{\boldsymbol{\ell}}\; e^{\hat{\mathbf{K}}x}\vec{\mathbf{R}}\,(\mathbf{I}_S \otimes \boldsymbol{a}/T)}{\ell^{\triangle}\vec{\boldsymbol{\ell}}\left(\mathbb{1}_{S_-} \otimes \boldsymbol{a}/T\right) + \int_{y=0}^{\infty} \ell^{\triangle}\vec{\boldsymbol{\ell}}\; e^{\hat{\mathbf{K}}y}\vec{\mathbf{R}}dy\,(\mathbb{1}_N \otimes \boldsymbol{a}/T)}. \qquad (81)
$$

Simplifying with $\ell^{\triangle}$, using $\int_{y=0}^{\infty} e^{\hat{\mathbf{K}}y}dy = -\hat{\mathbf{K}}^{-1}$ and $1/C = \vec{\boldsymbol{\ell}}\left(\mathbb{1}_{S_-} \otimes \boldsymbol{a}/T\right) - \vec{\boldsymbol{\ell}}\;\hat{\mathbf{K}}^{-1}\vec{\mathbf{R}}\,(\mathbb{1}_S \otimes \boldsymbol{a}/T)$, we obtain (73) and (74). □

4.3 Transient analysis with NILT

4.3.1 NILT when A is diagonalizable

To approximate the transient behaviour of the MFM at time T based on its LT in (45) and (46), we write

$$\boldsymbol{\ell}(T) \approx \boldsymbol{\ell}_N(T) = \sum_{n=1}^{N} \frac{\eta_n}{T} \boldsymbol{\ell}^* \left(\frac{\beta_n}{T}\right) \tag{82}$$

$$= \sum_{n=1}^{N} \frac{\eta_n}{T} \left(\boldsymbol{\pi}_+ \boldsymbol{\Psi}^* \left(\frac{\beta_n}{T}\right) + \boldsymbol{\pi}_-\right) \left(s\mathbf{I} - \mathbf{Q}_- - \mathbf{Q}_{-+} \boldsymbol{\Psi}^* \left(\frac{\beta_n}{T}\right)\right)^{-1},$$

$$\boldsymbol{p}(T,x) \approx \boldsymbol{p}_N(T,x) = \sum_{n=1}^{N} \frac{\eta_n}{T} \boldsymbol{p}^* \left(\frac{\beta_n}{T}, x\right) \tag{83}$$

$$= \sum_{n=1}^{N} \frac{\eta_n}{T} \left(\boldsymbol{\pi}_+ + \boldsymbol{\ell}^* \left(\frac{\beta_n}{T}\right) \mathbf{Q}_{-+}\right) e^{\mathbf{K}^* \left(\frac{\beta_n}{T}\right) x} \left[\mathbf{R}_+^{-1}, -\boldsymbol{\Psi}^* \left(\frac{\beta_n}{T}\right) \mathbf{R}_-^{-1}\right].$$

4.3.2 NILT when A is not diagonalizable

Similar to the CTMC case, when $\mathbf{A}$ is not diagonalizable we utilize Theorem 1 for which we need to compute $\boldsymbol{L}^*(-\mathbf{A}/T) = \int_0^\infty \boldsymbol{\ell}(t) \otimes e^{\mathbf{A}t/T} dt$ and $\boldsymbol{P}^*(-\mathbf{A}/T, x) = \int_0^\infty \boldsymbol{p}(t,x) \otimes e^{\mathbf{A}t/T} dt$.

Theorem 8. *$\boldsymbol{L}^*(-\mathbf{A}/T)$ and $\boldsymbol{P}^*(-\mathbf{A}/T, x)$ can be computed as*

$$\boldsymbol{L}^*(-\mathbf{A}/T) = -\left((\boldsymbol{\pi}_+ \otimes \mathbf{I}_N)\bar{\boldsymbol{\Psi}} + (\boldsymbol{\pi}_- \otimes \mathbf{I}_N)\right)\left(\mathbf{Q}_- \oplus \mathbf{A}/T + (\mathbf{Q}_{-+} \otimes \mathbf{I}_N)\bar{\boldsymbol{\Psi}}\right)^{-1},$$

$$\boldsymbol{P}_+^*(-\mathbf{A}/T, x) = ((\boldsymbol{\pi}_+ \otimes \mathbf{I}_N) + \boldsymbol{L}^*(-\mathbf{A}/T)(\mathbf{Q}_{-+} \otimes \mathbf{I}_N))e^{\bar{\mathbf{K}}x}(\mathbf{R}_+^{-1} \otimes \mathbf{I}_N),$$

$$\boldsymbol{P}_-^*(-\mathbf{A}/T, x) = -((\boldsymbol{\pi}_+ \otimes \mathbf{I}_N) + \boldsymbol{L}^*(-\mathbf{A}/T)(\mathbf{Q}_{-+} \otimes \mathbf{I}_N))e^{\bar{\mathbf{K}}x}\bar{\boldsymbol{\Psi}}(\mathbf{R}_-^{-1} \otimes \mathbf{I}_N).$$

Proof. The proof follows the same pattern as the one of Theorem 4. We introduce the transient MFM with generator $\bar{\mathbf{Q}} = \mathbf{Q} \oplus \mathbf{A}/T$ and $\bar{\mathbf{R}} = \mathbf{R} \otimes \mathbf{I}_N$ and apply Theorem 6. □

From Theorem 1 and 8, the NILT based approximation of $\boldsymbol{\ell}(T)$ and $\boldsymbol{p}(T,x)$ are

$$\boldsymbol{\ell}(T) \approx \boldsymbol{\ell}_N(T) = (\mathbf{I}_1 \otimes \boldsymbol{\alpha})\boldsymbol{L}^*(-\mathbf{A}/T)(\mathbf{I}_{S_-} \otimes \boldsymbol{a}/T), \tag{84}$$

$$\boldsymbol{p}(T,x) \approx \boldsymbol{p}_N(T,x) = (\mathbf{I}_1 \otimes \boldsymbol{\alpha})\boldsymbol{P}^*(-\mathbf{A}/T, x)(\mathbf{I}_S \otimes \boldsymbol{a}/T), \tag{85}$$

where $\mathbf{I}_1 \otimes \boldsymbol{\alpha}$ $(= 1 \otimes \boldsymbol{\alpha} = \boldsymbol{\alpha})$ is written to refer to the Kronecker product structure of Theorem 1 and $\mathbf{P}^*(-\mathbf{A}/T, x) = [\mathbf{P}_+^*(-\mathbf{A}/T, x), \mathbf{P}_-^*(-\mathbf{A}/T, x)]$.

From Theorem 8, we can also compute the normalizing constant of Theorem 7.

Lemma 2. *The normalizing constant of Theorem 7 satisfies*

$$C = \frac{1}{\vec{\boldsymbol{\ell}}\big(\mathbb{1}_{S_-} \otimes \boldsymbol{a}/T\big) - \overrightarrow{\boldsymbol{\ell}}\ \hat{\mathbf{K}}^{-1}\overrightarrow{\mathbf{R}}\,(\mathbb{1}_S \otimes \boldsymbol{a}/T)} = 1.$$

Proof. From Theorem 8 and (84), we have

$$\boldsymbol{\ell}_N(T)\mathbb{1}_{S_-} = (\mathbf{I}_1 \otimes \boldsymbol{\alpha})\boldsymbol{L}^*(-\mathbf{A}/T)(\mathbf{I}_{S_-} \otimes \boldsymbol{a}/T)\mathbb{1}_{S_-} =$$
$$-\left((\boldsymbol{\pi}_+ \otimes \boldsymbol{\alpha})\bar{\boldsymbol{\Psi}} + (\boldsymbol{\pi}_- \otimes \boldsymbol{\alpha})\right)\left(\mathbf{Q}_- \oplus \mathbf{A}/T + (\mathbf{Q}_{-+} \otimes \mathbf{I}_N)\bar{\boldsymbol{\Psi}}\right)^{-1}(\mathbb{1}_{S_-} \otimes \boldsymbol{a}/T) =$$
$$\vec{\boldsymbol{\ell}}\big(\mathbb{1}_{S_-} \otimes \boldsymbol{a}/T\big)\,.$$

Similarly, from (85) we have

$$\int_0^\infty \boldsymbol{p}_{N+}(T,x)dx\mathbb{1}_{S_+} = (\mathbf{I}_1 \otimes \boldsymbol{\alpha})\int_0^\infty \mathbf{P}_+^*(-\mathbf{A}/T,x)dx(\mathbf{I}_{S_+} \otimes \boldsymbol{a}/T)\mathbb{1}_{S_+} =$$
$$\Big((\boldsymbol{\pi}_+ \otimes \boldsymbol{\alpha}) + \underbrace{(\mathbf{I}_1 \otimes \boldsymbol{\alpha})\boldsymbol{\ell}^*(-\mathbf{A}/T)}_{=\vec{\boldsymbol{\ell}}}(\mathbf{Q}_{-+} \otimes \mathbf{I}_N)\Big)\int_0^\infty e^{\bar{\mathbf{K}}x}dx(\mathbf{R}_+^{-1} \otimes \mathbf{I}_N)(\mathbb{1}_{S_+} \otimes \boldsymbol{a}/T) =$$
$$\overrightarrow{\boldsymbol{\ell}}(-\bar{\mathbf{K}})^{-1}(\mathbf{R}_+^{-1} \otimes \mathbf{I}_N)(\mathbb{1}_{S_+} \otimes \boldsymbol{a}/T),$$

and

$$\int_0^\infty \boldsymbol{p}_{N-}(T,x)dx\mathbb{1}_{S_-} = (\mathbf{I}_1 \otimes \boldsymbol{\alpha})\int_0^\infty \mathbf{P}_-^*(-\mathbf{A}/T,x)dx(\mathbf{I}_{S_-} \otimes \boldsymbol{a}/T)\mathbb{1}_{S_-} =$$
$$-\overrightarrow{\boldsymbol{\ell}}(-\bar{\mathbf{K}})^{-1}\bar{\boldsymbol{\Psi}}(\mathbf{R}_-^{-1} \otimes \mathbf{I}_N)(\mathbb{1}_{S_-} \otimes \boldsymbol{a}/T),$$

where $\overrightarrow{\boldsymbol{\ell}}$ is defined in (72). Using the relation

$$\int_0^\infty \boldsymbol{p}_N(T,x)dx\mathbb{1}_S = \left[\int_0^\infty \boldsymbol{p}_{N+}(T,x)dx, \int_0^\infty \boldsymbol{p}_{N-}(T,x)dx\right]\mathbb{1}_S =$$
$$\overrightarrow{\boldsymbol{\ell}}(-\bar{\mathbf{K}})^{-1}\underbrace{\left[(\mathbf{R}_+^{-1} \otimes \mathbf{I}_N), -\bar{\boldsymbol{\Psi}}(\mathbf{R}_-^{-1} \otimes \mathbf{I}_N)\right]}_{=\overrightarrow{\mathbf{R}}}(\mathbb{1}_{S_-} \otimes \boldsymbol{a}/T),$$

we can write

$$1 = \int_0^\infty f_N(t/T)/Tdt = \int_0^\infty f_N(t/T)/T\underbrace{\left(\boldsymbol{\ell}(t)\mathbb{1}_{S_-} + \int_0^\infty \boldsymbol{p}(t,x)dx\mathbb{1}_S\right)}_{=1}dt$$
$$= \boldsymbol{\ell}_N(T)\mathbb{1}_{S_-} + \int_0^\infty \boldsymbol{p}_N(T,x)dx\mathbb{1}_S = \vec{\boldsymbol{\ell}}\big(\mathbf{I}_{S_-} \otimes \boldsymbol{a}/T\big) - \overrightarrow{\boldsymbol{\ell}}\ \hat{\mathbf{K}}^{-1}\overrightarrow{\mathbf{R}}\,(\mathbb{1}_S \otimes \boldsymbol{a}/T)\,.$$

□

5 Conclusion

The paper proves the identity of the NILT and the random clock based analysis of CTMCs and MFMs when the same MEWF is used.

This identity leads to a new interpretation of the two analysis approaches. The properties of the analysis methods based on NILT and random clock do not depend on the approach, but they depend on the applied MEWF. Historically, MEWFs with alternating signs were used for NILT and non-negative MEWFs for random clock based analysis, which resulted in different perceptions of the two approaches.

Due to the identity of the approaches, the remaining open problem of the transient analysis Markov modulated stochastic processes is to find the appropriate MEWF. An additional research goal is to prove that the identity of NILT and clock based transient analysis extends to other stochastic processes.

References

[1] J. Abate, G. L. Choudhury, and W. Whitt. An introduction to numerical transform inversion and its application to probability models. In *Computational Probability*, pages 257–323. Springer US, Boston, MA, 2000.

[2] J. Abate and W. Whitt. A Unified Framework for Numerically Inverting Laplace Transforms. *INFORMS Journal on Computing*, 18(4):408–421, 2006.

[3] S. Ahn and V. Ramaswami. Transient analysis of fluid flow models via stochastic coupling to a queue. *Stochastic Models*, 20(1):71–101, 2004.

[4] S. Ahn and V. Ramaswami. Transient analysis of fluid models via elementary level-crossing arguments. *Stochastic Models*, 22(1):129–147, 2006.

[5] N. Akar, O. Gursoy, G. Horvath, and M. Telek. Transient and first passage time distributions of first and second-order multi-regime Markov fluid queues via ME-fication. *Methodology and Computing in Applied Probability (MCAP)*, 23:1257–1283, 2021.

[6] D. Aldous and L. Shepp. The least variable phase type distribution is Erlang. *Stochastic Models*, 3:467–473, 1987.

[7] N. Bean, G. Nguyen, and F. Poloni. Doubling algorithms for stationary distributions of fluid queues: A probabilistic interpretation. *Performance Evaluation*, 125:1–20, 2018.

[8] N. Bean, M. O'Reilly, and P. Taylor. Algorithms for the Laplace-Stieltjes transforms of first return times for stochastic fluid flows. *Methodology and Computing in Applied Probability*, 10:381–408, 2008.

[9] I. I. Hirchman and D. V. Widder. *The convolution transform*. Princeton University Press, Princeton, 1955.

[10] R. Horn and G. Piepmeyer. Two applications of the theory of primary matrix functions. *Linear Algebra and its Applications*, 361:99–106, 2003.

[11] G. Horváth, I. Horváth, and M. Telek. High order concentrated matrix-exponential distributions. *Stochastic Models*, 36(2):176–192, 2020.

[12] I. Horváth, G. Horváth, S. A.-D. Almousa, and M. Telek. Numerical inverse Laplace transformation using concentrated matrix exponential distributions. *Performance Evaluation*, 137:102067, 2020.

[13] A. Mészáros and M. Telek. Concentrated matrix exponential distributions with real eigenvalues. *Probability in the Engineering and Informational Sciences*, page 117, 2021.

[14] V. Ramaswami. Matrix analytic methods for stochastic fluid flows. In *International Teletraffic Congress*, pages 1019–1030, Edinburg, 1999.

[15] V. Ramaswami, D. G. Woolford, and D. A. Stanford. The Erlangization method for Markovian fluid flows. *Annals of Operations Research*, 160(1):215–225, 2008.

[16] H. Stehfest. Algorithm 368: Numerical Inversion of Laplace Transforms [D5]. *Commun. ACM*, 13(1):47–49, 1970.

[17] A. Talbot. The Accurate Numerical Inversion of Laplace Transforms. *IMA Journal of Applied Mathematics*, 23(1):97–120, 1979.

[18] B. Van Houdt and C. Blondia. Approximated transient queue length and waiting time distributions via steady state analysis. *Stochastic Models*, 21(2-3):725–744, 2005.

[19] J. Van Velthoven, B. Van Houdt, and C. Blondia. Simultaneous transient analysis of QBD Markov chains for all initial configurations using a level based recursion. In *Fourth International Conference on the Quantitative Evaluation of Systems (QEST 2007)*, pages 79–90, 2007.